Pathways and export of Greenland Sea Water

Tor Eldevik[1]

Nansen Environmental and Remote Sensing Center, Bergen, Norway

Fiammetta Straneo

Woods Hole Oceanographic Institution, Woods Hole, Massachusetts, USA

Anne Britt Sandø[1]

Nansen Environmental and Remote Sensing Center, Bergen, Norway

Tore Furevik[1]

Geophysical Institute, University of Bergen, Norway

The dense water that overflows the Greenland–Scotland Ridge from the Nordic Seas is a major source for the deep waters of the North Atlantic. An advective-diffusive model, with its current deduced from the data archive of a high resolution general circulation model, has been set up to describe the spreading of Greenland Sea Water through the Nordic Seas to the overflows. A diversity of flow regimes, e.g., positive and negative NAO, can be modelled by this flexible approach. There are large differences between the simulated cases, and they are predominantly due to the variability of the internal circulation of the Nordic Seas. The varying role played by the Jan Mayen Current is particularly striking. Model evaluation is done against the observed spreading of the tracer sulphur hexafluoride that was purposefully released in the central Greenland Sea in 1996. The model ocean compares very well with this unique field experiment.

To appear in the AGU monograph *Climate Variability of the Nordic Seas*, Drange et al., Eds., 8/9/2004.

1. INTRODUCTION

The overflows from the Nordic Seas are a major source for the deep waters of the North Atlantic, and thus important contributors to the Atlantic Meridional Overturning Circulation. Where the overflow water is formed, and how, is still a matter of debate. Proposed mechanisms involve: open-ocean convection, primarily in the Greenland Sea, dense water produced on the Arctic shelves during the winter [for both, see *Aagaard et al.*, 1985], and the gradual transformation of Atlantic

Water while it undergoes its cyclonic loop in the boundary current around the periphery of the Nordic Seas–Arctic Ocean [*Mauritzen*, 1996a,b].

While drifter measurements over the last decade have provided new insight into the surface flow of the Nordic Seas [*Jakobsen et al.*, 2003; *Orvik and Niiler*, 2002; *Poulain et al.*, 1996], less is known of the intermediate and deep water flow. The general picture, based on rather sparse deep-water measurements [cf. *Hansen and Østerhus*, 2000] and diagnostic calculations using climatological hydrography and wind stress curl as input [*Nøst and Isachsen*, 2003], reveal an intermediate and deep water flow that is generally in the same direction as the surface flow, with northward flow west of Norway and southward flow east of Greenland. Also, there is cyclonic circulation within the sub-basins: the Greenland Sea, the Iceland Sea, and the Norwegian and Lofoten basins of the Norwegian Sea. Figure 1 is a synthesis of these characteristics.

Figure 1

The Greenland Sea is a 'hot spot' for open ocean convection [*Alekseev et al.*, 2001; *Marshall and Schott*, 1999]. The spreading of intermediate and deep water from the central Greenland Sea to the Greenland–Scotland Ridge is the object of our study. It is inspired by *Straneo et al.'s* [2003] description of the spreading of Labrador Sea Water. Their advective-diffusive model is here set up for the Nordic Seas intermediate water (IW). The stationary model current is deduced from an eddy-permitting general circulation model (GCM) covering the region [*Hátún et al.*, 2004]. The four different current regimes of figures 2–4 are considered: the mean over the whole GCM simulation period (1951–2000), the flows related to negative and positive phases of the North Atlantic Oscillation, and the circulation of recent years (1997–2000). In the summer of 1996 a patch of the tracer sulphur hexafluoride (SF_6) was purposefully released in the central Greenland Sea [*Watson et al.*, 1999]. The monitoring of its spreading since the release provides a unique benchmark for evaluating the model.

figures 2–4

The goal of this study is to investigate the different pathways of the Greenland Sea Water (GSW) within the Nordic Seas, and the export of GSW at the overflows to the North Atlantic. The paper is organized as follows: the advective-diffusive model and the (proxy) current data are presented in section 2, and the model concept is illustrated by the flow and tracer spreading generated by the mean IW current. The model is evaluated in section 3, where the comparison with recent SF_6 tracer data suggests that the concept is suitable for the study. The flows related to weak and strong at-

mospheric forcing are presented in the following section. The different model pathways and exports are compared and discussed in section 5. The importance of the Jan Mayen Current relative to the East Greenland Current, and of the Faroe–Shetland Channel overflow relative to the Denmark Strait are addressed in particular. The concluding remarks of section 6 summarize the paper.

2. THE MODEL OCEAN

A very simple and flexible concept is used for our study: the Greenland Sea Water (GSW) is assumed to be a passive tracer in an advective-diffusive model ocean. The tracer is advected by a stationary horizontal current $\mathbf{U} = \mathbf{U}(x, y)$, and mixed by an eddy diffusivity tensor $\underset{\sim}{\boldsymbol{\kappa}} = \underset{\sim}{\boldsymbol{\kappa}}(x, y)$, representing the flow at intermediate depths in the Nordic Seas. The evolution of the GSW in the basin is then governed by

$$\frac{\partial \phi}{\partial t} + \mathbf{U} \cdot \nabla \phi = \nabla \cdot (\underset{\sim}{\boldsymbol{\kappa}} \cdot \nabla)\phi, \tag{1}$$

where $\phi = \phi(x, y, t)$ is the concentration per unit area.

The model was originally set up by *Straneo et al.* [2003] to describe the spreading of Labrador Sea Water (LSW) in the subpolar North Atlantic. Their model flow field was deduced from float data, and hydrographic data were used to identify different scenarios of LSW generation, and thereby initialize the tracer. The different pathways and timescales for LSW spreading identified in their study compare well with observations, thus supporting both the choice of the model fields and, in general, the approach used to address the spreading of the convectively formed LSW. The model also proved to be a valuable tool with which to quantify the relative importance of the different pathways.

In this study, the general approach of *Straneo et al.* [2003] is applied to the spreading of GSW with some important differences. First of all, the mean flow field is model derived. This allows for a variety of mean flows to be utilized to investigate the spreading in different climate regimes (unlike Straneo et al. who kept the flow field constant). Finally, the ongoing SF_6 experiment conducted in the Greenland Sea provides an ideal ('real') passive tracer against which to test the validity of our approach.

2.1. The Current Data

The stationary horizontal current field and diffusivity prescribed to equation (1) should ideally be based on in situ observations (which is the case for the Labrador Sea study). The Nordic Seas hydrography have been sampled for more than a century [e.g., *Helland-Hansen and*

Nansen, 1909; *Furevik et al.*, 2002], and drifters have in recent years revealed the flow of the surface layer in great detail [e.g., *Orvik and Niiler*, 2002]. Intermediate and deep current measurements are nevertheless sparse [*Blindheim and Østerhus*, 2004; *Hansen and Østerhus*, 2000], and can therefore not be used as a basis for our model of the intermediate waters of the Nordic Seas. We therefore construct proxy current data from the output of the high resolution, synoptically forced GCM of *Hátún et al.* [2004], which is a version of the Miami Isopycnic Coordinate Ocean Model (MICOM [*Bleck et al.*, 1992]). Their regional model simulation covers the North Atlantic Ocean and the Nordic Seas (30°N–80°N) for the years 1948-2000. The model has 25 isopycnic layers below its mixed layer, and a horizontal resolution of about 20 km in the Nordic Seas region. At the lateral boundaries of the region model, the different model components are relaxed towards weekly output from a global model of the same type, with half the resolution [*Furevik et al.*, 2002].

Even with an ideally sampled GCM data archive available (model insufficiencies aside), one still has to decide on which subset to derive the velocity data from. We have chosen to average over the intermediate water (IW), herein defined to be the water between 500 and 1500 m depth. Where the ocean depth is less than 1500 m, the average velocities are weighted consistent with the reduced thickness. The choice is partly pragmatic. The advection-diffusion model describes tracer conservation by a non-divergent horizontal flow. As oceanic circulation is predominantly horizontal, the 'geometrically' averaged current is close to non-divergent. The upper limit of 500 m assures that the data in general are collected well below the mixed layer. The Nordic Seas are characterized by relatively cold water below this level, which also corresponds to the typical sill depth of the Greenland–Scotland Ridge [*Hansen et al.*, 2001]. It is still sufficiently shallow to account for the overflows of the Denmark Strait (DS, 620 m deep) and the Faroe–Shetland Channel (FSC, 840 m deep). The lower limit of 1500 m exceeds the ocean depth only in the very vicinity of the overflows. The deeper flow is presumably still well accounted for: the vertical stratification and velocity shear at depth in the Nordic Seas are quite weak in hydrographic data [e.g., *Blindheim and Østerhus*, 2004; *Hopkins*, 1991], as well as in the observational based diagnostics of *Nøst and Isachsen* [2003], and in GCMs (e.g., the one at hand). Furthermore, convection has since the 1980s only been ventilating the Greenland Sea to intermediate depths [cf. *Dickson et al.*, 1996; *Watson et al.*, 1999], and the SF_6

that the model is evaluated against is found in the IW (cf. section 3).

A qualitatively different, and maybe more intuitive alternative would be to sample an isopycnic layer (or range) representative of the wintertime ventilation in the Greenland Sea. This option was discarded as an isopycnic definition is not straightforward when linking the GSW with the overflows. The water below a few hundred meters in the central Greenland Sea has a potential density $\sigma_\theta > 28.05$ [*ESOP2*, 1999], while the bulk of the overflowing waters in the FSC and DS are lighter than this [cf. *Fogelqvist et al.*, 2003; *Girton et al.*, 2001]. This is also the case for the waters of the GCM.

2.2. The Mean Pathways

The mean IW velocity field and streamlines from the GCM simulation period 1951–2000 (the 1948–1950 spin-up is not used) is shown in Figure 2. The GCM current is interpolated to the 10 km × 10 km grid of the advection-diffusion solver. For details on the numerical solver of equation (1), the reader is referred to *Straneo et al.* [2003]. The domain is as seen in Figure 2. Note that no streamlines cross the Iceland–Faroe Ridge as it is shallower than 500 m. Although the IW current was defined with some care, the flow is not strictly mass conserving. A relatively small flux correction has to be added at the open boundary to make $\mathbf{U}$ conservative. For all the simulations described herein, the correction was prescribed uniformly over the inflowing part of the Fram Strait (FS), the open boundary to the north. The overflows then remain as in the original GCM current data, and one does not run the risk of strangling the relative weak outflowing branch in the eastern FS. These considerations nevertheless have little practical importance. When prescribing the relaxation elsewhere, there were only marginal quantitative changes, no qualitative.

The IW streamlines of Figure 2 reproduce the general pattern from Figure 1. The cyclonic circulation covering the Norwegian and Lofoten basins is particularly pronounced in the model flow. It may possibly be too strong, but a similar pattern is present in the diagnosis of *Nøst and Isachsen* [2003]. It should also be noted that the pattern is relatively persistent over the GCM simulation period (cf. Figure 3), and therefore should stand out in the mean.

The regional model and the corresponding coarser global versions (with grid focus on the Arctic Mediterranean), should be state of the art for GCM systems covering the Nordic Seas. The GCMs' spreading of active [*Furevik et al.*, 2002] and passive [*Gao et al.*, 2004]

tracers, as well as their Atlantic-Nordic Seas exchanges [*Hátún et al.*, 2004; *Nilsen et al.*, 2003], have all been evaluated favourably against observations. The export fluxes in the case of the advection-diffusion model are 0.8 Sv (1 Sv = $10^6 \mathrm{m}^3\mathrm{s}^{-1}$) through the DS and 1.4 Sv through the FSC. Recent overflow estimates based on observations are 0.6 Sv [*Girton et al.*, 2001] and 1.7 Sv [*Hansen and Østerhus*, 2000], respectively. The referred DS flux is for the densest part of the overflow, $\sigma_\theta \geq 28.0$. The net model IW influx through the FS, per definition the sum of the DS and FSC fluxes, is 2.2 Sv.

Open ocean convection in the Nordic Seas is predominantly associated with the Greenland Sea Gyre. Although the gyre is a dynamical feature, it is normally understood to (roughly) coincide with the 3500 m isobath in the central Greenland Sea [e.g., *Bönisch et al.*, 1997; *Marshall and Schott*, 1999]. The topographical definition of the gyre agrees well with the mean circulation (cf. figures 2 and 3d), but less so for the other cases (figures 3a–c). This is addressed further in the discussion of section 5. For a straightforward comparison between the cases, this isobath was still used as the initial boundary of the model GSW in all the simulations (but the one evaluated against SF_6 data).

The initial tracer distribution together with the mean IW current and the constant nominal diffusivity (see below) were prescribed to equation (1) to produce the GSW spreading of Figure 5. The tracer is advected and diffused from the gyre area. By year 3 (Figure 5b) it has reached the FS to the north, and two distinct branches point to the two overflows via the East Greenland Current (EGC) and the Jan Mayen Current (JMC). The EGC branch has reached the DS by year 5 (Figure 5c), where some tracer is deflected eastward to join the tracer advected by the JMC to overflow at the FSC (Figure 5d). The different straits and currents are indicated in Figure 1. The mean picture will be further characterized and compared with the other simulations in the next sections.

Figure 5

2.3. The Model Diffusion

The diffusive contribution to the tracer's evolution represents the action of mesoscale eddies. In regions of open-ocean convection, these eddies will primarily have one of two origins: 1) the instability of the convective water mass or, 2) the instability of the boundary current surrounding the convective region. The distinction between the two is important. While the former eddies are temporally and spatially tied to convection [e.g., *Jones and Marshall*, 1993,1997], the latter are less directly tied to a distinct convective event and more to

the mean gradient between the convective region and the more buoyant currents around it. Recent studies from the Labrador Sea, an open-ocean convection region that is thought to be quite similar to the Greenland Sea [e.g., *Marshall and Schott*, 1999], show growing evidence that spreading of the convectively formed water is a slow process dominated by the mean eddy fluxes due to type 2) instability as opposed to the seasonal, convectively-generated turbulence. For example, *Lilly et al.* [1999] have shown, using mooring data, that the small-scale, high frequency turbulence associated with convection is typically short-lived, rapidly decaying one to two months after convection. Similarly, *Straneo* [2004] showed how Labrador Sea Water export occurs mostly at a uniform rate, persisting even in years when no convection occurred (and hence is not directly tied to that year's convection). Several recent model studies also argue that the dense water export is dominated by the continuous exchange of properties between the site of (intermittent) convection and the surrounding boundary current [*Katsman et al.* 2004; *Spall* 2004]. Given this, the assumption in this study (as in *Straneo et al.* [2003]) is that the lateral diffusion of the passive tracer is dominated by the mean eddy fluxes and not by the turbulence associated with convection. Effectively, this amounts to assuming a separation of timescales between the short-lived convection and the slower spreading of the dense water formed.

The eddy diffusivity is assumed constant in the four case studies herein, $\underset{\sim}{\boldsymbol{\kappa}} = \kappa \underset{\sim}{I}$, and set to the nominal value $\kappa = 100\,\mathrm{m^2 s^{-1}}$. *Poulain et al.* [1996] estimate an eddy length scale for the Nordic Seas in the range 10–40 km from their surface layer drifters. With $\kappa \sim u'L$ and an eddy velocity scale $u' = 1\,\mathrm{cm\,s^{-1}}$ (same as the mean flow, cf. Figure 2), an estimate of the IW diffusivity related to mesoscale eddies is then 100–400 $\mathrm{m^2\,s^{-1}}$. A constant value representing the basin average should then be in the very low range of this.

Although the velocity field of the eddy-*permitting* GCM has been argued an adequate substitute for lacking in situ measurements, it is probably rather unsuited for a detailed quantification of $\underset{\sim}{\boldsymbol{\kappa}}$ and its spatial distribution. The mesoscale eddies, whose mixing the eddy diffusivity represents, are mostly parameterized and not resolved by the 20 km horizontal grid of the GCM. If one nevertheless calculates the root-mean-square zonal and meridional "eddy" velocities from the weekly sampled GCM archive, using the difference between the weekly values and the 1951–2000 mean, Figure 6 is the result. The largest values are, as one would expect, associated with regions of strong gradients in the mean flow, and

Figure 6

of large variability (cf. Figure 3). The basin averages are 0.7 and 0.9 cm s^{-1} in the two respective directions.

For an eddy length scale of 10 km, the above velocities correspond to eddy diffusivities in units of 10^2 m^2 s^{-1}. To check the model's sensitivity to anisotropic and spatially inhomogeneous diffusion, we performed an experiment using these GCM derived eddy velocities and an eddy length scale of 10 km. A snapshot from this experiment is shown in Figure 7a. The spreading pattern differs only in details from that of the reference experiment (Figure 5c). This is consistent with *Straneo et al.* [2003] who found that the impact of the eddy diffusivity's spatial variability was quite limited in their study of the Labrador Sea. A second sensitivity experiment was done by simply doubling the reference homogeneous diffusivity to $\kappa = 200\,m^2s^{-1}$. The value is probably too large to represent a basin average, but the GSW evolution in this case (Figure 7b) is still very similar to the reference. As one would expect there are lower peak concentrations and weaker gradients.

Figure 7

2.4. A Note on Model Relevance

The fundamental spreading properties of the Nordic Seas flow topology is at the heart of the advection-diffusion approach. Distinct cases are easily set up within the framework, e.g., the restriction to the IW and the different four-year-mean flows of the next section. A pertinent question at this stage is nevertheless: how suited is an advective-diffusive model for the present study? The model current is deduced from the data archive of a GCM. One could argue that the tracer spreading should be modelled directly by the GCM. This is not really an option. A ten year "online" tracer realisation would consume 4000 CPU-hours on a supercomputer (as of 2004). The model ocean described by equation (1), which is one way of doing "off-line" tracer studies based on the GCM, covers the same time span in 1 hour on a laptop computer. Furthermore, the comparison of simulated and observed SF_6 spreading and export (cf. section 3) supports the use of this model in investigating the IW pathways.

3. MODEL EVALUATION: THE SF_6 EXPERIMENT

In August 1996, 320 kg of the passive tracer sulphur hexafluoride (SF_6) was released at intermediate depth in the central Greenland Sea [*ESOP2*, 1999; *Watson et al.*, 1999]. The main objective of the (still ongoing) experiment is very much the same as ours: to track the GSW from its potential generation site in the gyre area

along the pathways of the Nordic Seas, into the neighbouring oceans. This gives important insight to the basin's present physical oceanography. More particular, the continuous monitoring of the tracer since the release [*Messias et al.*, 2004; *Olsson et al.*, 2004] provides a unique benchmark for ocean models. The relevance of the tracer experiment to our particular model is further emphasized by the fact that the maximum concentration of SF_6 is generally measured in the IW part of the water column. Thus, as a direct evaluation of the advection-diffusion approach and of the GCM-generated model field, we here present an experiment simulating the spreading of SF_6.

The 1997–2000 mean flow field (the GCM velocity archive ends with the year 2000) is chosen as that most representative of the 'SF_6-years'. The streamlines are shown in Figure 3a. It does show the general IW patterns of figures 1 and 3d, but there are features more emphasized in the late 1990s current. Note particularly that the streamlines following the JMC, diverting into the Norwegian Sea east of Jan Mayen, are more pronounced. It indicates that the JMC is more important for the export through the FSC in this case. This is confirmed by the pattern described by the model tracer and the concentrations at the overflows presented below.

For the specific comparison of model and SF_6 observations, the model tracer was initialized consistent with the August 1996 release. A snapshot of that case, corresponding to the summer of 2002, is shown in Figure 8a. The black rectangle centered at 1.5°W, 75.25°N is the release site. Two large scale surveys of SF_6 were done in 2002 as parts of the EU project TRACTOR. The first was from April 20 to June 6 (*R/V Oden*) and the second from May 30 to July 1 (*R/V Knorr*). The stars in the figure are the hydrographic stations occupied by the *Oden* and the circles are those occupied by the *Knorr*. The numbers from 1 to 9 mark the start of the section identified by the given number. *Messias et al.* [2004] have analysed and synthesised these observations. Their SF_6 inventory (with the background subtracted) is displayed in Figure 8b together with the model concentration interpolated to the hydrographic stations. The stations are equally spaced along the horizontal axis where the numbers indicate the start of the different sections. The general agreement between model and field data is very good both with respect to the magnitude and to the relative distribution of the concentration. The model seems to be off in parts of sections 7 and 8, where the model has two high concentration anomalies. These are the one extending from the

Figure 8

central Greenland Sea to the Lofoten Basin just crossing section 7, and the one in the eastern Norwegian Basin intersected to the south by 8. This suggests that the model recirculation in the Lofoten and Norwegian basins (cf. Figure 3a) may be somewhat too strong; see also the discussion on this for the mean flow in subsection 2.2. The evolution of SF_6 concentration predicted by the model in the central FSC is shown in Figure 9. The time history observed by *Olsson et al.* [2004] in the Faroe Bank Channel is included. There is a remarkable agreement in arrival and build-up time, and peak concentration between the two.

Figure 9

4. PHASES OF POSITIVE AND NEGATIVE NAO

The basic experiment described in subsection 2.2, using the long-term averaged GCM velocity, is meant to represent the average timescales and spreading pathways for GSW. However, the Nordic Seas are characterized by large interannual variability that is often associated with that of the North Atlantic Oscillation (NAO), the leading mode of the North Atlantic sea level pressure pattern. It represents the shift of atmospheric mass between the Icelandic Low and Azores High, and the associated index (Figure 4) is a measure for the strength of the westerlies [*Hurrell*, 1995]. During a phase of positive NAO index, with stronger than normal westerlies, there is enhanced cyclonic atmospheric circulation in the Nordic Seas, with strengthened southwesterlies in the southeast and strengthened northerlies in the west. On short time scales (∼months), the direct effect of a positive NAO is to increase the wind stress curl over the Nordic Seas. The associated divergence in the Ekman transports and sea level changes will favour an enhanced barotropic cyclonic circulation within the Nordic Seas and sub-basins [*Furevik and Nilsen*, 2004]. On longer time scales (∼years), heat and freshwater fluxes associated with the NAO can alter the thermohaline structure of the ocean, and lead to slow baroclinic adjustment processes. The effect of this is much more difficult to model, and may involve propagation of Rossby waves and advection of anomalies with the mean circulation from remote regions [*Furevik and Nilsen*, 2004; *Visbeck et al.*, 2003].

Variations in the NAO, and in particular the change from weak westerlies in the 1960s to extremely strong westerlies in the 1990s, have been found to correlate with changes in an abundance of physical, ecological, and even economical parameters in the North Atlantic and Nordic Seas regions [cf. *Hurrell et al.*, 2003; *Marshall et al.*, 2001]. For the Nordic Seas area, reduced

deep water formation in the Greenland Sea, increased transport of heat towards the Arctic Ocean, and a general freshening of the intermediate waters, are all notifiable changes in the recent oceanographic conditions that have been related to the NAO. See *Blindheim and Østerhus* [2004], and *Furevik and Nilsen* [2004] for reviews.

The NAO index for the time period under consideration is displayed in Figure 4. The 1960s were characterized by negative NAO, but the index has been predominantly positive since 1972 with an all-time high in 1989 (the index goes back to 1864). We construct a positive NAO case from the 1989–1992 mean of the GCM IW circulation, and a negative one from the 1962–1965 mean. Within the four-year intervals, the index is quite persistent. Also, a four-year period does in general cover the time it takes from the tracer is released in the Greenland Sea until it arrives at the overflows (cf. Table 1 and Figure 11), and is consistent with the definition of the SF_6 case.

The intensified circulations of the sub-basins and gyres of the Nordic Seas, characteristic of the strong NAO+ forcing, are clearly seen in Figure 3b. The circulation of the Greenland Sea is particularly strong in the positive phase. This is also the case for the streamlines connecting the Greenland and Norwegian Sea directly, shortcutting the GSW's journey to the FSC. It is quite similar to the late 1990s (Figure 3a), but the closed circulations are in general substantially stronger during NAO+. This should be expected as the late 1990s were characterized by a positive index of only moderate magnitude.

The energetic NAO+ case is contrasted with the expected weaker NAO– flow of 1962–1965 in Figure 3c. Compared with the others, the NAO– case is more similar to the mean flow. One difference, however, concerns the way the northern basin connects with the overflows: the Jan Mayen Current and the shortcut to the Norwegian Sea have practically vanished, and the meridional flow in the Norwegian Basin is much less pronounced. The different spreading of the passive tracer, initially restricted by the 3500 m isobath, for the two distinct forcing regimes is shown in Figure 10. The negative index yields the slower spreading and practically all the overflowing tracer is delivered by the East Greenland Current as expected from the streamfunctions. In the positive case, the spreading is much faster and the JMC has a dominant role.

Figure 10

5. DISCUSSION

The variability displayed in Figure 3 is striking, both in flow strength and pathways. The JMC shortcut directly from the Greenland Sea to the Norwegian Sea clearly stands out in the late 1990s and NAO+, while it is weak or almost non-existent in the other two. Another related feature that is highly variable is the internal circulation of the Greenland Sea. The mean case displays a Greenland Sea gyre coinciding roughly with the 3500 m isobath. Across the Greenland Fracture Zone to the northeast, there is a similar closed circulation in the Boreas Basin. This basin has been associated on a smaller scale with many of the same convective characteristics as the central Greenland Sea [cf. *Johannessen et al.*, 2004]. The negative NAO forcing moves the gyre slightly to the east. The strong wind stress curl of the positive NAO case (and the late 1990s) characteristically spins up the circulation, but also offsets it some 300 km to the south where it is restricted by the Jan Mayen Fracture Zone and the Mohns Ridge that separate the Greenland Basin from the Norwegian and the Lofoten basins, respectively. Such an extensive translation is not traditionally associated with the Greenland Sea Gyre. Although it is possible that the GCM is too sensitive at depth to changes in the wind forcing, we argue that these differences could be representative of the real system since the wind stress curl is a decisive parameter in setting the gyre [e.g., *Dickson et al.*, 1996]. Also, the mean diagnostics of *Nøst and Isachsen* [2003] produce a gyre very similar to that of Figure 3d. Both gyres have relatively weak flows and are 'correctly' placed over the Greenland Abyssal Plain. Their low inertia and the weak topographic gradients below make them vulnerable to changes in the forcing. Furthermore, hydrographic sections in the Greenland Sea are mostly taken at, or close to 75°N [e.g., *Bönisch et al.*, 1997; *ESOP2*, 1999]. Unless a survey has sufficient three-dimensional coverage, it is often impossible to decide whether a section goes through the center or the periphery of a certain structure. For example, all the gyres of Figure 3 do intersect 75°N and would all leave the 'Greenland Sea Gyre-signature' of doming isopycnals there.

The evolution of GSW concentration at the overflows for all the regimes is shown in Figure 11, and the salient features are summarized in Table 1. For this comparison the late 1990s flow was initialized like the others. The according spreading of GSW was qualitatively like that of NAO+ (not shown). The arrival time at the DS is similar in all the cases. This is due to the fact that the pathway taken by the GSW exported at the DS is the

Figure 11

Table 1

EGC (e.g., Figure 5). The following build-up times are less similar, and the peak concentrations vary almost by a factor of five. This can be understood from the varying course taken by the tracer to the FSC. In the negative NAO and mean cases the tracer comes via the EGC, and the part that does not leave at the DS travels southeast through the Iceland and Norwegian Seas to exit at the FSC roughly two years later. The setting of the positive NAO and 'SF_6-years' is completely different (cf. Figure 10). The bulk of the tracer exported through the FSC is provided through the shortcut of the JMC, taking the GSW directly from the Greenland to the Norwegian Sea. Much faster arrival and larger peak concentration at the FSC is the result. The concentrations in the outflow of the eastern FS are included in Figure 11 for completeness. What stands out in the GSW export to the Arctic is the mean case, followed by the NAO+. It is noteworthy that the above similarity of the mean and NAO– cases, and of the late 1990s and NAO+, is absent.

There is, maybe surprisingly, practically the same net IW flux through the model domain for the mean (2.2 Sv) and the NAO+/NAO– flows (2.3/2.2 Sv). The 2.6 Sv of the late 1990s is slightly stronger. Furthermore, the division of the influx between the overflows is the same (±1%) for all cases, with 36% to the DS and 64% to the FSC. The large differences between the four regimes is thus not a result of varying fluxes through the open boundaries, but solely due to the variability of the internal circulation of the Nordic Seas. This emphasizes that a key factor for the (model) export of GSW to the North Atlantic is the role of the JMC. The Jan Mayen Current has previously been associated with substantial interannual variability, both from the monitoring of the "Odden" ice tongue [*Comiso et al.*, 2001], and measurements of the bottom current [*Østerhus and Gammelsrød*, 1999]. As these observations concern the surface and near-bottom layers, no quantitative comparison is attempted with the IW of the model JMC.

The overflow fluxes referred to above are consistent (as they should be) with the transports in *Nilsen et al.'s* [2003] coarser version of the MICOM GCM. Their analysis suggests a basic balance between the variability of the net inflow through the FSC and the net outflow through the DS (integrating over the total water column). The GCM fluxes and the analysis is supported by what the authors can infer from relevant observations.

6. CONCLUDING REMARKS

An advective-diffusive model of the Nordic Seas has been set up to address the spreading of Greenland Sea Water. The model currents were taken, in lack of in situ observations, from the data archive of a high resolution GCM. A comparison of the model results with observations collected following the 1996 SF_6 tracer release in the central Greenland Sea lends credibility both to the velocity field from the GCM as well as to the approach utilized (cf. figures 8, 9).

The variable spreading under different regimes and, in particular, distinct phases of the NAO, are here presented. The variability between the different flow cases is striking, both in streamline patterns and in tracer distribution (cf. figures 3, 10, 11). It is found that the variability in tracer pathways and export reflects changes both in the pattern and the strength of the internal circulation of the Nordic Seas, and not in the fluxes of the overflows. The Jan Mayen Current plays a key role in the different spreading. When it is weak relative to the East Greenland Current (the mean and NAO– cases), practically all of the overflowing tracer follows the latter. When the Jan Mayen Current is strong (the late 1990s and NAO+ cases), the Greenland Sea Water's pathway to the Faroe-Shetland Channel is cut short by the Jan Mayen Current.

Notation

CPU	central processing unit
DS	Denmark Strait
EGC	East Greenland Current
FS	Fram Strait
FSC	Faroe–Shetland Channel
GCM	general circulation model
GSW	Greenland Sea Water
IW	intermediate water
JMC	Jan Mayen Current
LSW	Labrador Sea Water
MICOM	Miami Isopycnic Coordinate Ocean Model
NAO	North Atlantic Oscillation
SF_6	sulphur hexafluoride

Acknowledgments. The authors thank Marie-José Messias and Anders Olsson for making the SF_6-data available through the EU TRACTOR project, and the three reviewers for their helpful comments. TE was supported by TRACTOR (EVK2-2000-00080) and the Norwegian Research Council project ProClim (155923/700), FS by NSF #0240978, ABS by the research programme West-Nordic Ocean Climate of the Nordic Council of Ministers, and TF by the Norwegian Research Council project NOClim II (155972/720). This is contribution Nr. A69 from the Bjerk-

nes Centre for Climate Research.

REFERENCES

Aagaard, K., J. H. Swift, and E. C. Carmack, Thermohaline circulation in the Arctic Mediterranean Seas, *J. Geophys. Res.*, *90, C3*, 4833–4846, 1985.

Alekseev, G. V., O. M. Johannessen, A. A. Korablev, V. V. Ivanov, and D. M. Kovalevsky, Interannual variability of water masses in the Greenland Sea and the adjacent areas, *Polar Res.*, *20*, 201–208, 2001.

Bleck, R., C. Rooth, D. Hu, and L. T. Smith, Salinity-driven thermocline transients in a wind- and thermocline-forced isopycnic coordinate model of the North Atlantic, *J. Phys. Oceanogr.*, *22*, 1486–1505, 1992.

Blindheim, J., and S. Østerhus, The Nordic Seas main oceanographic features, To appear in *Climate Variability of the Nordic Seas*, H. Drange, T. M. Dokken, T. Furevik, R. Gerdes, and W. Berger, Eds., Geophysical Monograph Series, AGU, 2004.

Bönisch, G., J. Blindheim, J. L. Bullister, P. Schlosser, and D. W. R. Wallace, Long-term trends of temperature, salinity, density, and transient tracers in the central Greenland Sea, *J. Geophys. Res.*, *102, C8*, 18553–18571, 1997.

Comiso, J. C., P. Wadhams, L. T. Pedersen, and R. A. Gersten, Seasonal and interannual variability of the Odden ice tongue and a study of environmental effects, *J. Geophys. Res.*, *106, C5*, 9093–9116, 2001.

Dickson, B., J. Lazier, J. Meincke, P. Rhines, and S. J., Long-term coordinated changes in the convective activity of the North Atlantic, *Prog. Oceanog.*, *38*, 241–295, 1996.

ESOP2 Group, *The thermohaline circulation in the Greenland Sea, ESOP2/MAST3 Final scientific report*, University of Bergen, Jansen, E. and Opheim, V., Eds., 1999.

Fogelqvist, E., J. Blindheim, T. Tanhua, S. Østerhus, E. Buch, and F. Rey, Greenland-Scotland overflow studied by hydro-chemical multivariate analysis, *Deep Sea Res. I*, *50*, 73–102, 2003.

Furevik, T., M. Bentsen, H. Drange, J. Johannessen, and A. Korablev, Temporal and spatial variability of the sea surface salinity in the Nordic Seas, *J. Geophys. Res.*, *107, C12*, DOI 10.1029/2001JC001118, 2002.

Furevik, T., and J. E. Ø. Nilsen, Large-scale atmospheric circulation variability ind its impact on the Nordic Seas ocean climate- a review, To appear in *Climate Variability of the Nordic Seas*, H. Drange, T. M. Dokken, T. Furevik, R. Gerdes, and W. Berger, Eds., Geophysical Monograph Series, AGU, 2004.

Gao, Y., H. Drange, M. Bentsen, and O. M. Johannessen, Simulating transport of non-Chernobyl ^{137}Cs and ^{90}Sr in the North Atlantic-Arctic region, *J. Environ. Radioactivity*, *71*, 1–16, 2004.

Girton, J. B., T. B. Sanford, and R. H. Käse, Synoptic sections of the Denmark Strait Overflow, *Geophys. Res. Lett.*, *28*, 1619–1622, 2001.

Hansen, B., and S. Østerhus, North Atlantic–Nordic Seas exchanges, *Prog. Oceanog.*, *45*, 109–208, 2000.

Hansen, B., W. R. Turrell, and S. Østerhus, Decreasing overflow from the Nordic seas into the Atlantic Ocean through the Faroe Bank channel since 1950, *Nature*, *411*, 927–930, 2001.

Hátún, H., A. B. Sandø, H. Drange, and M. Bentsen, Seasonal to decadal variations in the Faroe-Shetland inflow

waters, To appear in *Climate Variability of the Nordic Seas*, H. Drange, T. M. Dokken, T. Furevik, R. Gerdes, and W. Berger, Eds., Geophysical Monograph Series, AGU, 2004.

Helland-Hansen, B., and F. Nansen, *The Norwegian Sea, its physical oceanography based upon the Norwegian Researches 1900–1904*, Report on Norwegian Fishery and Marine Investigations, Vol. 2, part 1, No. 2, Mallingske, Christiania, 390 pp., 1909.

Hopkins, T. S., The GIN Sea- A synthesis of its physical oceanography and literature review 1972-1985, *Earth Sci. Rev.*, *30*, 175–318, 1991.

Hurrell, J. W., Decadal trends in the North Atlantic Oscillation: Regional temperatures and precipitation, *Science*, *269*, 676–679, 1995.

Hurrell, J. W., Y. Kushnir, G. Ottersen, and M. Visbeck, editors, *The North Atlantic Oscillation: Climate Significance and Environmental Impact*, vol. 134 of *Geophysical monograph*, American Geophysical Union, 279 pp., 2003.

Jakobsen, P. K., M. H. Ribergaard, D. Quadfasel, T. Schmith, and C. W. Hughes, Near surface circulation in the northern North Atlantic as inferred from Lagrangian drifters: Variability from the mesoscale to interannual, *J. Geophys. Res.*, *108, C8*, DOI 10.1029/2002JC001554, 2003.

Johannessen, O. M., K. Lygre, and T. Eldevik, Convective chimneys and plumes in the northern Greenland Sea, To appear in *Climate Variability of the Nordic Seas*, H. Drange, T. M. Dokken, T. Furevik, R. Gerdes, and W. Berger, Eds., Geophysical Monograph Series, AGU, 2004.

Jones, H., and J. Marshall, Convection with rotation in a neutral ocean: a study of open-ocean deep convection, *J. Phys. Oceanogr.*, *23*, 1009–1039, 1993.

Jones, H., and J. Marshall, Restratification after deep convection, *J. Phys. Oceanogr.*, *27*, 2276–2287, 1997.

Katsman, C. A., M. A. Spall, and R. S. Pickart, Boundary current eddies and their role in the restratification of the Labrador Sea, *J. Phys. Oceanogr.*, *34*, 1967–1983, 2004.

Lilly, J. M., P. B. Rhines, M. Visbeck, R. Davis, J. R. N. Lazier, F. Schott, and D. Farmer, Observing deep convection in the Labrador Sea during 1994/95, *J. Phys. Oceanogr.*, *29*, 2065–2098, 1999.

Marshall, J., Y. Kushnir, D. Battisti, P. Chang, A. Czaja, R. Dickson, J. Hyrrell, M. McCartney, R. Saravanan, and M. Visbeck, North Atlantic climate variability: phenomena, impacts and mechanisms, *Int. J. Climatol.*, *21*, 1863–1898, 2001.

Marshall, J., and F. Schott, Open-ocean convection: observations, theory, and models, *Rev. Geophys.*, *37*, 1–64, 1999.

Mauritzen, C., Production of dense overflow waters feeding the North Atlantic across the Greenland-Scotland Ridge. Part 1: Evidence for a revised circulation scheme, *Deep Sea Res. I*, *43*, 769–806, 1996a.

Mauritzen, C., Production of dense overflow waters feeding the North Atlantic across the Greenland-Scotland Ridge. Part 2: An inverse model, *Deep Sea Res. I*, *43*, 807–835, 1996b.

Messias, M.-J., A. Watson, T. Johannessen, K. A. Olsson, W. M. Smethie, L. Anderson, S. Bacon, J.-C. Gascard, J. Olafsson, K. Oliver, J. Swift, F. Rey, K. Simonsen, J. R. Ledwell, and G. Budeus, The Greenland Sea Tracer

Experiment: Formation, spreading and dispersion of intermediate waters of the Greenland Sea, In preparation, 2004.

Nilsen, J. E. Ø., Y. Gao, H. Drange, T. Furevik, and M. Bentsen, Simulated North Atlantic–Nordic Seas water mass exchanges in an isopycnic coordinate OGCM, *Geophys. Res. Lett.*, *30*, DOI 10.1029/2002GL016597, 2003.

Nøst, O. A., and P. E. Isachsen, The large-scale time-mean ocean circulation in the Nordic Seas and Arctic Ocean estimated from simplified dynamics, *J. Mar. Res.*, *61*, 175–210, 2003.

Olsson, K. A., E. Jeansson, L. G. Anderson, B. Hansen, T. Eldevik, R. Kristiansen, M.-J. Messias, T. Johannessen, and A. J. Watson, Intermediate water from the Greenland Sea in the Faroe Bank Channel: spreading of released sulphur hexafluoride, Submitted to *Deep Sea Res.*, 2004.

Orvik, K. A., and P. Niiler, Major pathways of Atlantic water in the northern North Atlantic and Nordic Seas toward Arctic, *Geophys. Res. Lett.*, *29*, DOI 10.1029/2002GL015002, 2002.

Østerhus, S., and T. Gammelsrød, The abyss of the Nordic Seas is warming, *J. Climate*, *12*, 3297–3304, 1999.

Poulain, P.-M., A. Warn-Varnas, and P. P. Niiler, Near-surface circulation of the Nordic seas as measured by Lagrangian drifters, *J. Geophys. Res.*, *101, C8*, 18237–18258, 1996.

Spall, M. A., Boundary currents and water mass transformation in marginal seas, *J. Phys. Oceanogr.*, *34*, 1197–1213, 2004.

Straneo, F., The convective seasonal cycle of the Labrador Sea, Submitted to *J. Phys. Oceanogr.*, 2004.

Straneo, F., R. S. Pickart, and K. Lavender, Spreading of Labrador Sea water: an advective-diffusive study based on Lagrangian data, *Deep Sea Res. I*, *50*, 701–719, 2003.

Visbeck, M., E. Chassignet, R. Curry, T. Delworth, B. Dickson, and G. Krahmann, The ocean's response to North Atlantic Oscillation variability, in *The North Atlantic Oscillation: Climate Significance and Environmental Impact*, edited by Hurrell, J. W., Y. Kushnir, G. Ottersen, and M. Visbeck, vol. 134 of *Geophysical monograph*, pp. 113–146, American Geophysical Union, 2003.

Watson, A. J., M. J. Messias, E. Fogelqvist, K. A. Van Scoy, T. Johannessen, K. I. C. Oliver, D. P. Stevens, F. Rey, K. A. Tanhua, T. Olsson, F. Carse, K. Simonsen, J. R. Ledwell, E. Jansen, D. J. Cooper, J. A. Kruepke, and E. Guilyardi, Mixing and convection in the Greenland Sea from a tracer-release experiment, *Nature*, *401*, 902–904, 1999.

T. Eldevik and A. B. Sandø, Nansen Environmental and Remote Sensing Center, Thormøhlensgate 47, N-5006 Bergen, Norway. (e-mail: tor.eldevik@nersc.no; anne.britt.sandoe@nersc.no)

T. Furevik, Geophysical Institute, University of Bergen, Allégaten 70, N-5007 Bergen, Norway. e-mail: Tore.Furevik@gfi.uib.no

F. Straneo, Dept. of Physical Oceanography, Woods Hole Oceanographic Institute, MS 21, Woods Hole, MA 02543, USA. e-mail: fstraneo@whoi.edu

[1]Bjerknes Centre for Climate Research, Bergen, Norway

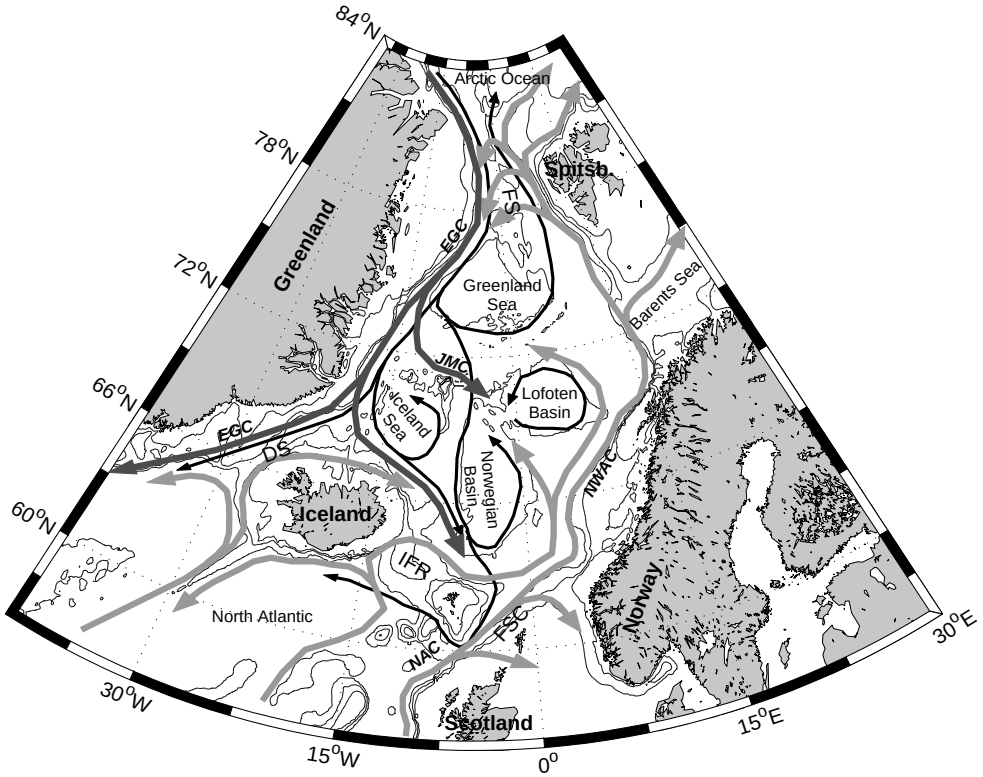

Figure 1. Sketch of the flow of the Nordic Seas. The thick arrows represent the surface flow of the Atlantic Water (light shade) and the Polar Water (dark shade), while the thin black arrows indicate the flow of intermediate and deep waters. See main text for references.

Figure 1. Sketch of the flow of the Nordic Seas. The thick arrows represent the surface flow of the Atlantic Water (light shade) and the Polar Water (dark shade), while the thin black arrows indicate the flow of intermediate and deep waters. See main text for references.

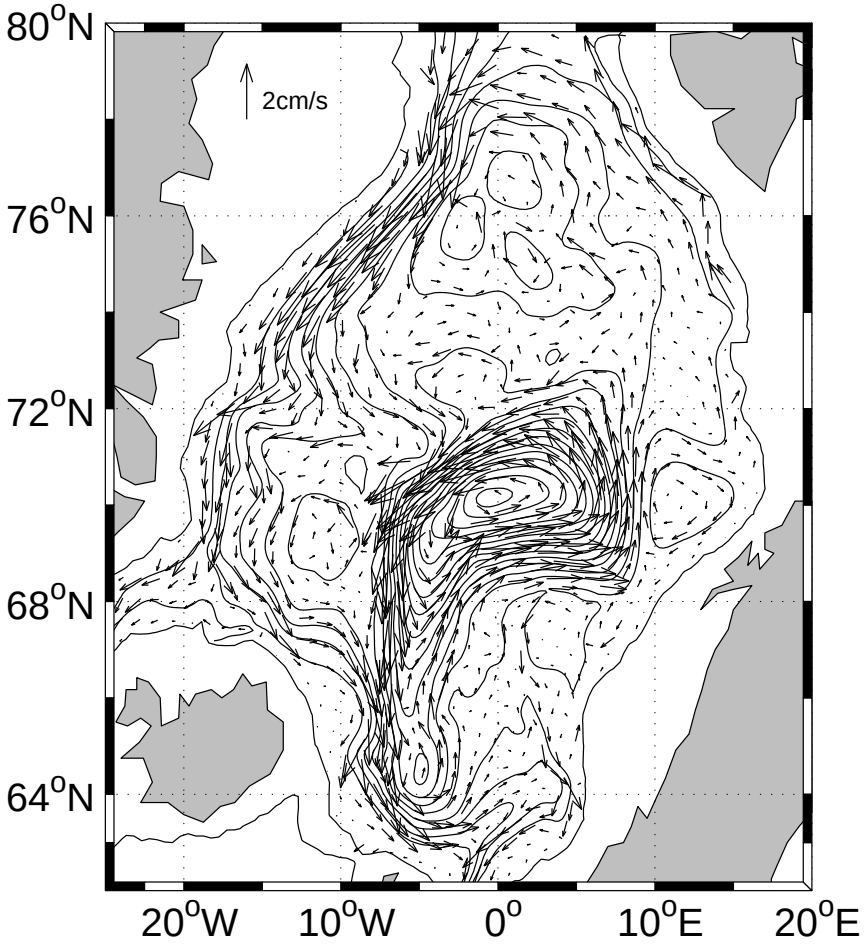

Figure 2. The mean (1951–2000) IW flow field from the GCM and the corresponding streamlines used by the advective-diffusive solver. Only a quarter of the vectors are shown. The spacing of streamlines corresponds to 0.25 Sv.

Figure 2. The mean (1951–2000) IW flow field from the GCM and the corresponding streamlines used by the advective-diffusive solver. Only a quarter of the vectors are shown. The spacing of streamlines corresponds to 0.25 Sv.

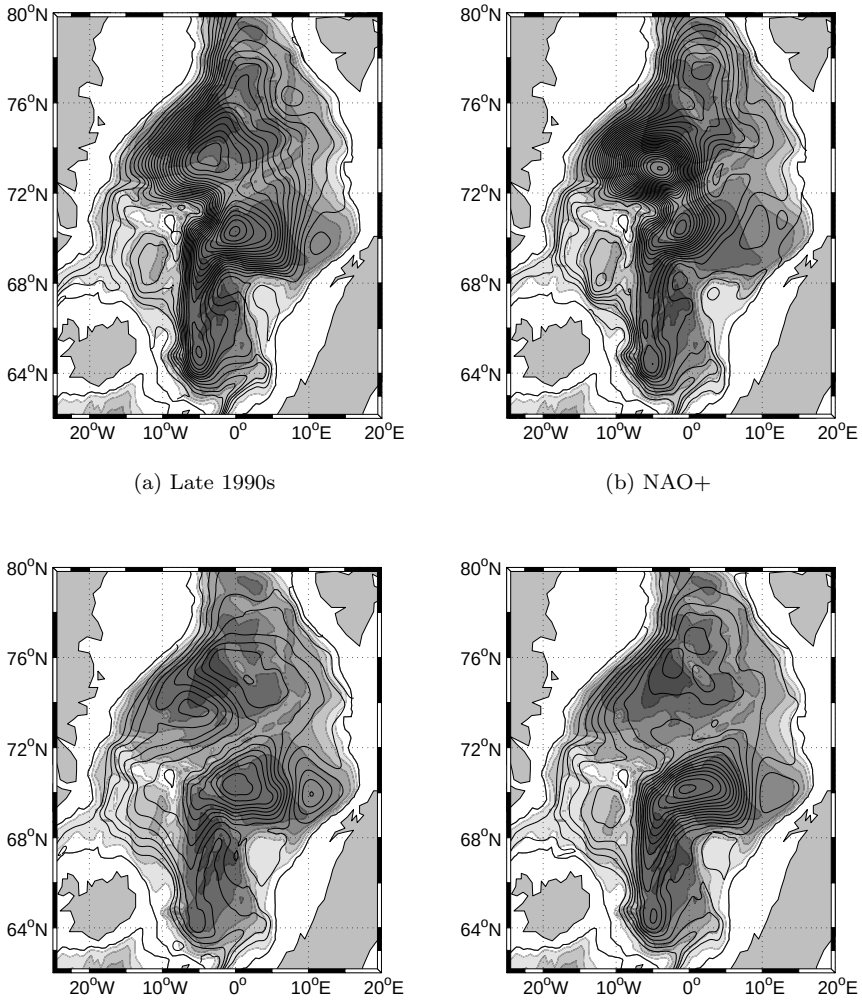

(a) Late 1990s (b) NAO+

(c) NAO– (d) Mean

Figure 3. The IW streamfunctions for the 'SF_6 years' 1997–2000 (a), and the periods of positive (1989–1992) and negative (1962–65) NAO (b,c). The mean (1951–2000) is given for reference in (d). The spacing of streamlines corresponds to 0.25 Sv, and the background grayscale give the bathymetry at 500 m intervals.

Figure 3. The IW streamfunctions for the 'SF_6 years' 1997–2000 (a), and the periods of positive (1989–1992) and negative (1962–65) NAO (b,c). The mean (1951–2000) is given for reference in (d). The spacing of streamlines corresponds to 0.25 Sv, and the background grayscale give the bathymetry at 500 m intervals.

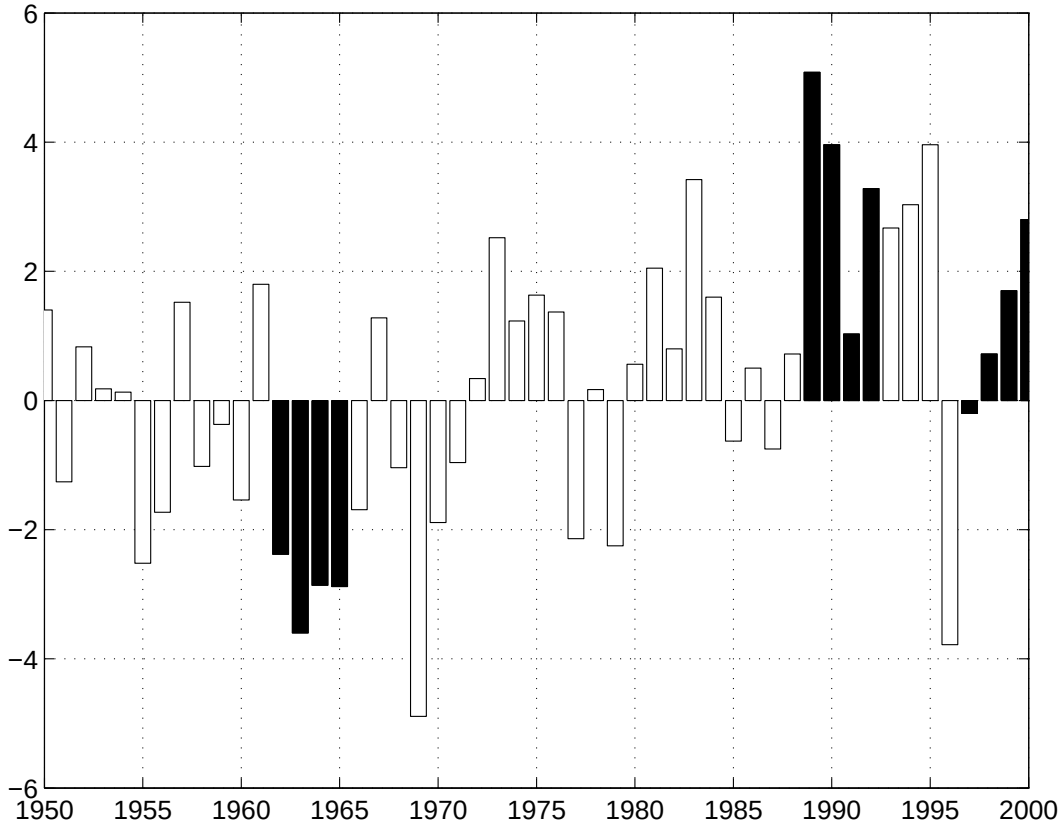

Figure 4. The winter NAO index (values taken from http://www.cgd.ucar.edu/~jhurrell/nao.html). The shading marks the three different four-year periods used.

Figure 4. The winter NAO index (values taken from http://www.cgd.ucar.edu/~jhurrell/nao.html). The shading marks the three different four-year periods used.

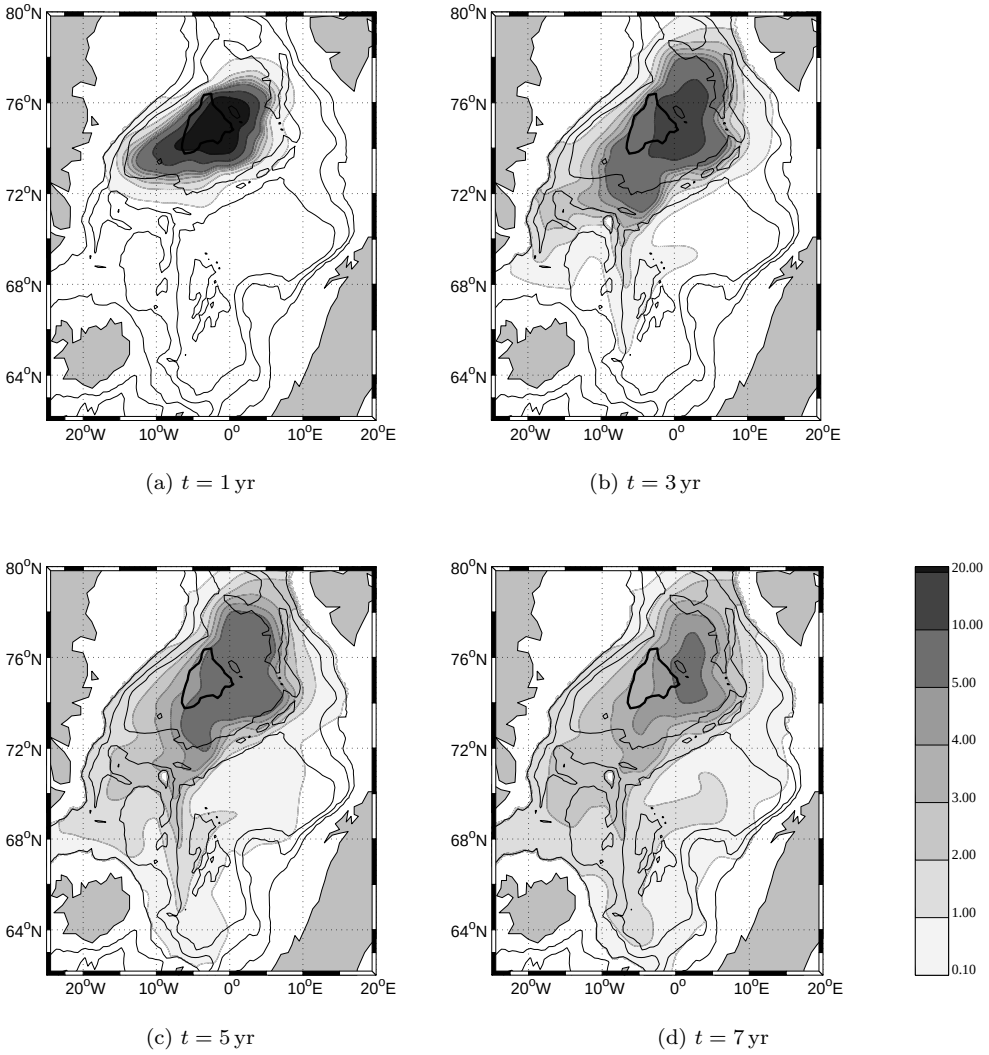

(a) $t = 1\,\mathrm{yr}$ (b) $t = 3\,\mathrm{yr}$

(c) $t = 5\,\mathrm{yr}$ (d) $t = 7\,\mathrm{yr}$

Figure 5. The spreading of tracer from the central Greenland Sea by the 1951–2000 mean IW flow. The background contours give the bathymetry at 1000 m intervals. Units in percent of the initial 100% concentration within the 3500 m isobath (thick line).

Figure 5. The spreading of tracer from the central Greenland Sea by the 1951–2000 mean IW flow. The background contours give the bathymetry at 1000 m intervals. Units in percent of the initial 100% concentration within the 3500 m isobath (thick line).

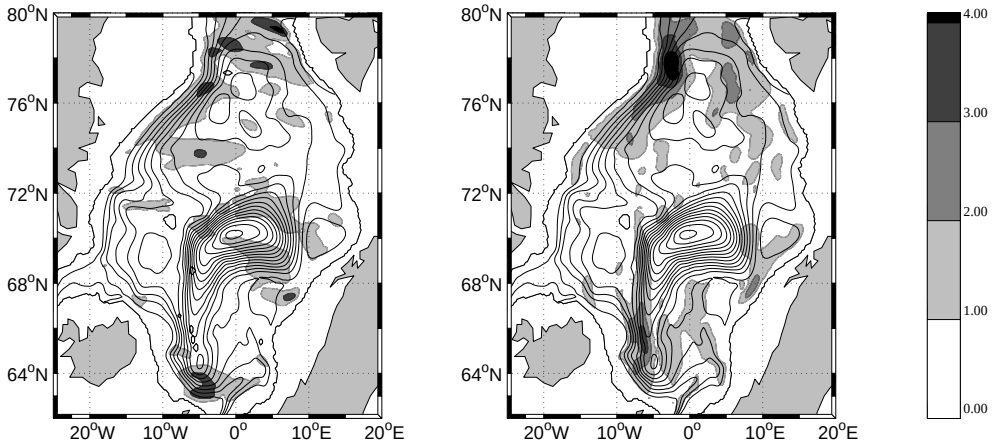

(a) Zonal (b) Meridional

Figure 6. The IW "eddy velocities" [$\mathrm{cm\,s^{-1}}$] calculated from the temporal variability of the GCM flow. The streamlines of the mean flow are also shown.

Figure 6. The IW "eddy velocities" [$\mathrm{cm\,s^{-1}}$] calculated from the temporal variability of the GCM flow. The streamlines of the mean flow are also shown.

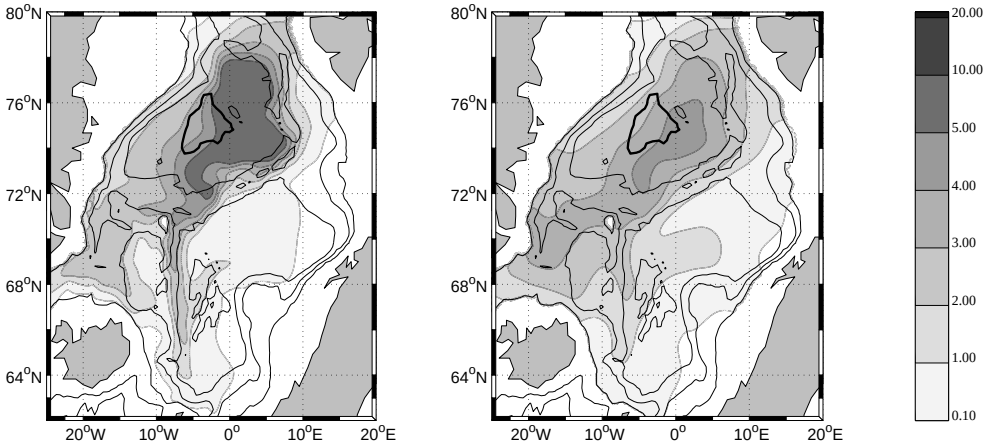

(a) $\boldsymbol{\kappa}(x, y)$ (b) $\kappa = 200\,\mathrm{m}^2\,\mathrm{s}^{-1}$

Figure 7. The spreading of tracer in the two eddy diffusion sensitivity experiments ($t = 5\,\mathrm{yr}$).

Figure 7. The spreading of tracer in the two eddy diffusion sensitivity experiments ($t = 5\,\mathrm{yr}$).

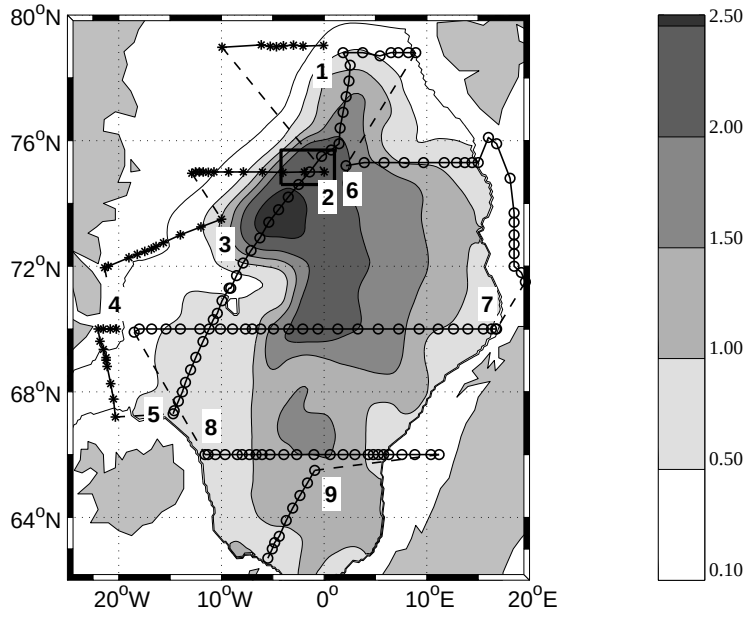

(a) Model tracer and hydrographic stations

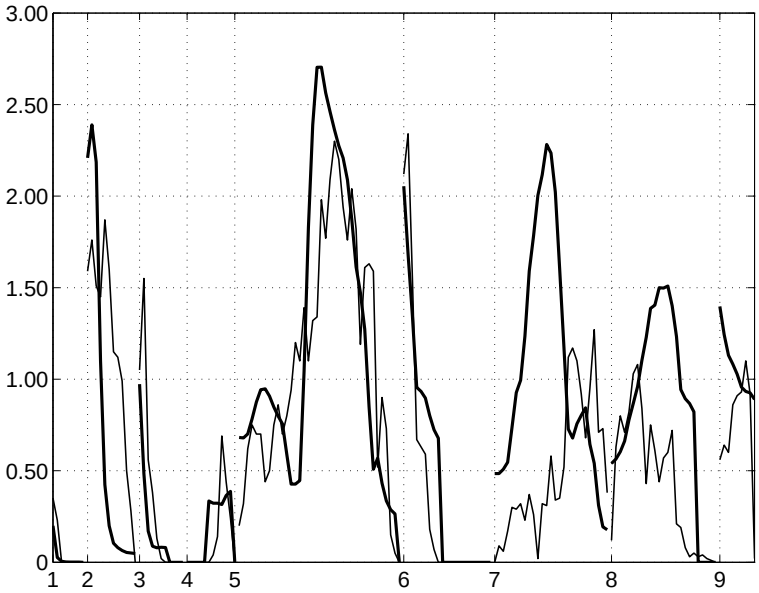

(b) Model versus observations

Figure 8. The modelled and observed SF_6 inventory [$\mathrm{nmol\,m^{-2}}$] for the summer 2002. The top panel (a) is the modelled distribution. Also shown are the hydrographic stations occupied by *R/V Oden* (stars) and *R/V Knorr* (circles). The model concentration of SF_6 (thick line) is compared with the observations (thin line) at the stations in (b), where the numbers along the horizontal axis give the start of the sections as indicated in (a). The observations are taken from *Messias et al.* [2004], and these authors should be cited when reference is made to the observational data.

Figure 8. The modelled and observed SF_6 inventory [$\mathrm{nmol\,m^{-2}}$] for the summer 2002. The top panel (a) is the modelled distribution. Also shown are the hydrographic stations occupied by *R/V Oden* (stars) and *R/V Knorr* (circles). The model concentration of SF_6 (thick line) is compared with the observations (thin line) at the stations in (b), where the numbers along the horizontal axis give the start of the sections as indicated in (a). The observations are taken from *Messias et al.* [2004], and these authors should be cited when reference is made to the observational data.

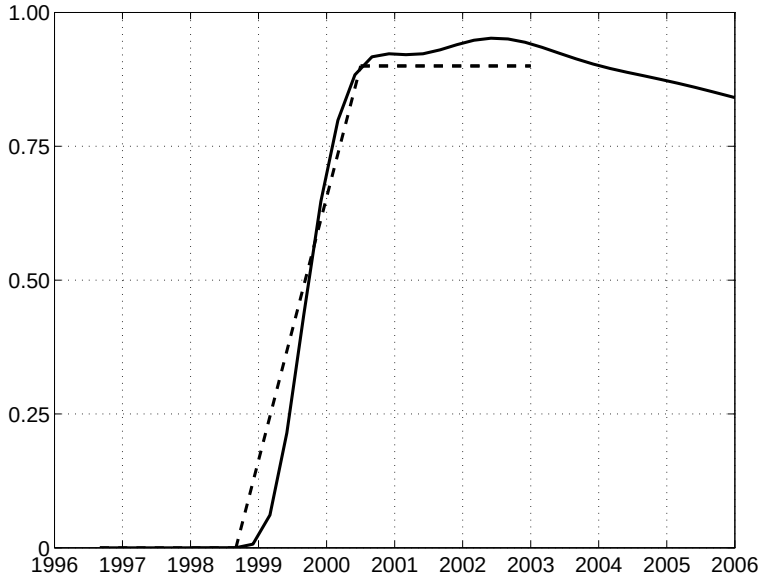

Figure 9. The model evolution of SF_6 concentration (in units of $\mathrm{nmol\,m^{-2}}$) in the central Faroe-Shetland Channel (solid curve). The broken line is the piecewise linear approximation to observations from the Faroe Bank Channel by *Olsson et al.* [2004].

Figure 9. The model evolution of SF_6 concentration (in units of $\mathrm{nmol\,m^{-2}}$) in the central Faroe-Shetland Channel (solid curve). The broken line is the piecewise linear approximation to observations from the Faroe Bank Channel by *Olsson et al.* [2004].

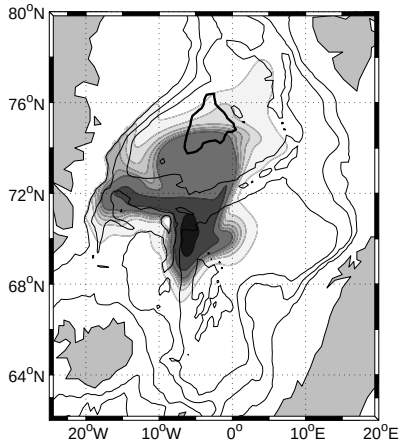

(a) NAO+, $t = 1\,\mathrm{yr}$

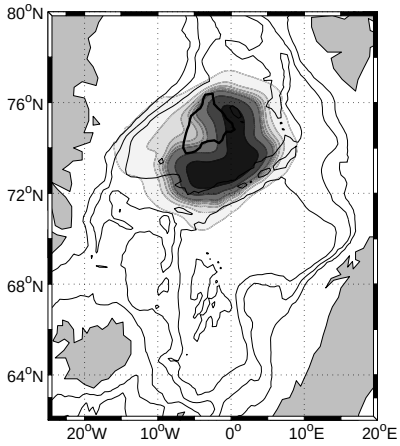

(b) NAO–, $t = 1\,\mathrm{yr}$

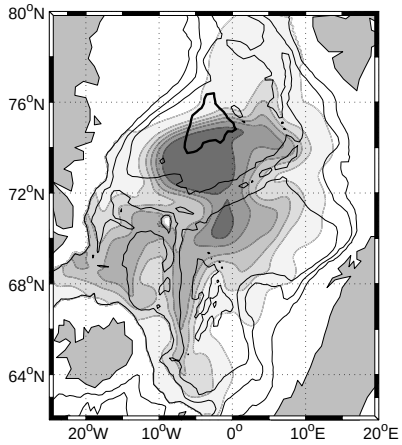

(c) NAO+, $t = 3\,\mathrm{yr}$

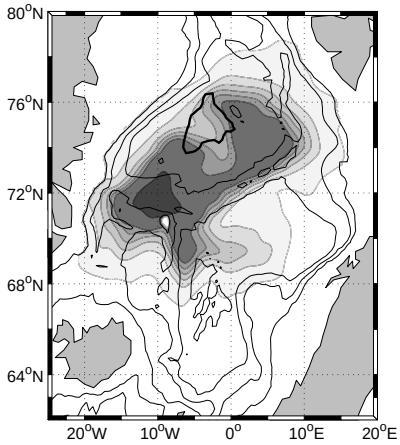

(d) NAO–, $t = 3\,\mathrm{yr}$

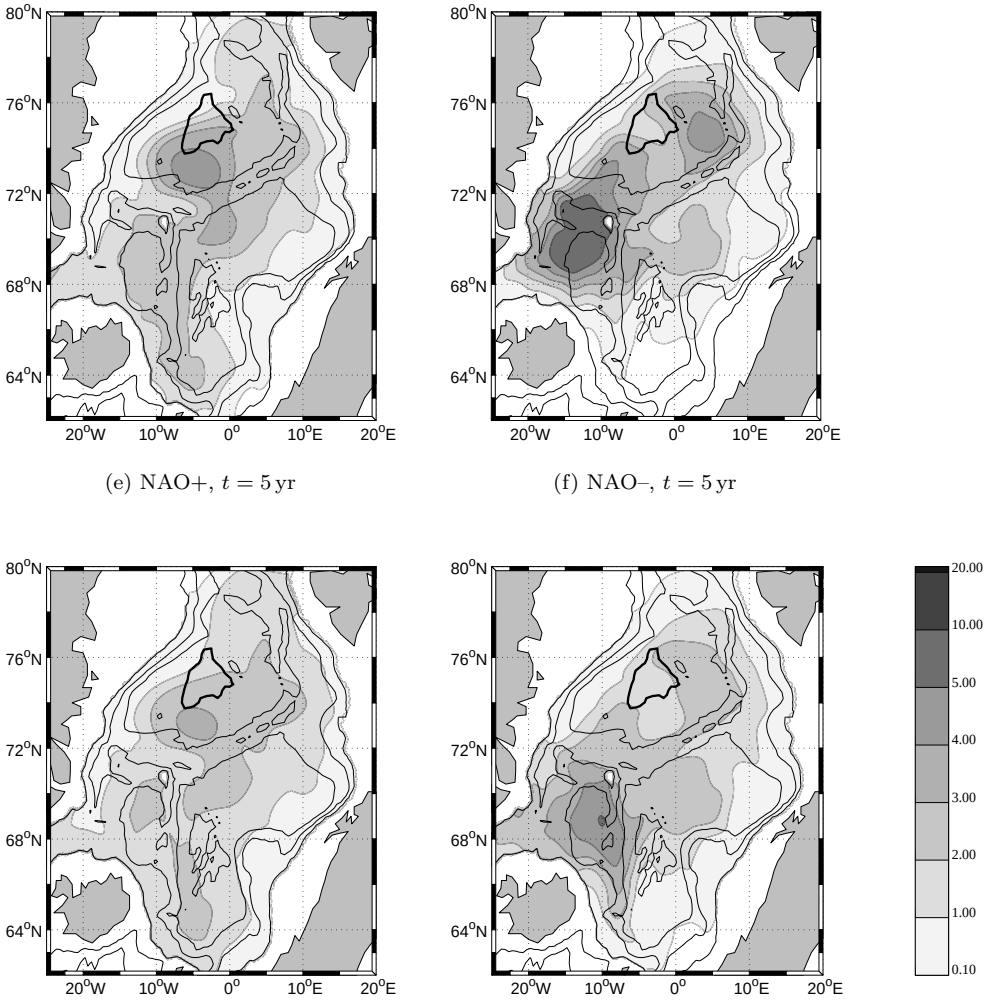

(e) NAO+, $t = 5\,\mathrm{yr}$

(f) NAO–, $t = 5\,\mathrm{yr}$

(g) NAO+, $t = 7\,\mathrm{yr}$

(h) NAO–, $t = 7\,\mathrm{yr}$

Figure 10. The spreading of GSW for positive NAO (1989-1992, left column) and negative (1962-1965, right), years 1, 3, 5 and 7 from top to bottom. Units in percent of the initial 100% concentration within the 3500 m isobath (thick line).

Figure 10. The spreading of GSW for positive NAO (1989-1992, left column) and negative (1962-1965, right), years 1, 3, 5 and 7 from top to bottom. Units in percent of the initial 100% concentration within the 3500 m isobath (thick line).

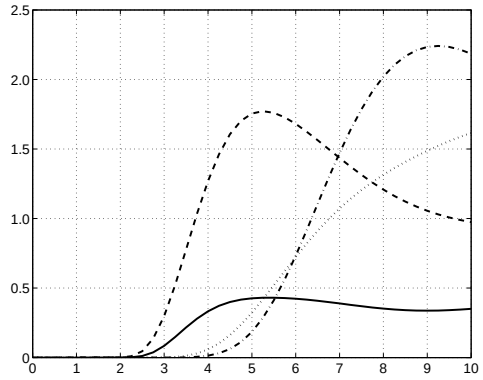

(a) Denmark Strait (DS)

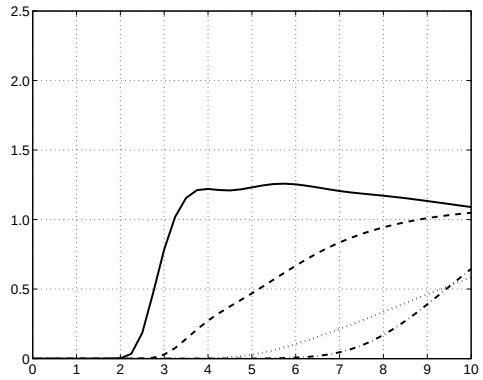

(b) Faroe–Shetland Channel (FSC)

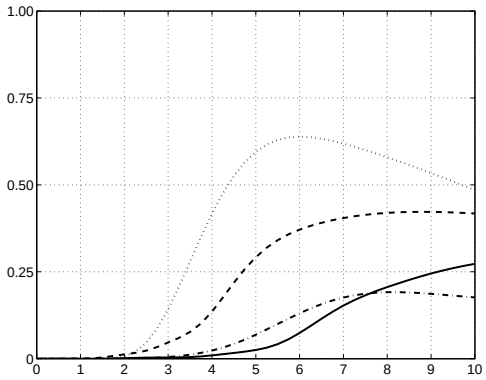

(c) Fram Strait (FS)

Figure 11. The evolution of tracer concentration (percent initial GSW) at the center of the two overflows and in the outflow in the eastern Fram Strait. The time is in years since release. The solid curves are the 'SF_6-years' (initialized like the others) and dashed/dash-dotted is positive/negative NAO. The mean evolution is given for reference by the dotted curves. Note that the range of the vertical axis in (c) is less than that of the others.

Figure 11. The evolution of tracer concentration (percent initial GSW) at the center of the two overflows and in the outflow in the eastern Fram Strait. The time is in years since release. The solid curves are the 'SF_6-years' (initialized like the others) and dashed/dash-dotted is positive/negative NAO. The mean evolution is given for reference by the dotted curves. Note that the range of the vertical axis in (c) is less than that of the others.

Table 1. The arrival time (T_{arr}), the following build-up time (ΔT_{bu}), and the associated peak tracer concentration (ϕ_{max}) at the two overflows. Bold font implies the shortest times and highest peak for each case. Units are years and percent of GSW.

	DS			FSC		
	T_{arr}	ΔT_{bu}	ϕ_{max}	T_{arr}	ΔT_{bu}	ϕ_{max}
Late 1990s	2.5	2.5	0.45	**2.0**	**2.0**	**1.25**
NAO+	**2.0**	**3.0**	**1.75**	2.5	7.5	1.05
NAO–	**4.0**	**5.0**	**2.25**	6.0	$\geq$4.0	$>$0.65
Mean	**3.0**	$\geq$7.0	**1.60**	4.5	$\geq$5.5	$>$0.60

PATHWAYS AND EXPORT OF GREENLAND SEA WATER

ELDEVIK ET AL.

PATHWAYS AND EXPORT OF GREENLAND SEA WATER

ELDEVIK ET AL.

PATHWAYS AND EXPORT OF GREENLAND SEA WATER

ELDEVIK ET AL.

PATHWAYS AND EXPORT OF GREENLAND SEA WATER

ELDEVIK ET AL.

PATHWAYS AND EXPORT OF GREENLAND SEA WATER

ELDEVIK ET AL.

PATHWAYS AND EXPORT OF GREENLAND SEA WATER

ELDEVIK ET AL.

PATHWAYS AND EXPORT OF GREENLAND SEA WATER

ELDEVIK ET AL.

PATHWAYS AND EXPORT OF GREENLAND SEA WATER

ELDEVIK ET AL.

PATHWAYS AND EXPORT OF GREENLAND SEA WATER

ELDEVIK ET AL.

PATHWAYS AND EXPORT OF GREENLAND SEA WATER

ELDEVIK ET AL.

PATHWAYS AND EXPORT OF GREENLAND SEA WATER

ELDEVIK ET AL.

PATHWAYS AND EXPORT OF GREENLAND SEA WATER

ELDEVIK ET AL.

PATHWAYS AND EXPORT OF GREENLAND SEA WATER

ELDEVIK ET AL.

PATHWAYS AND EXPORT OF GREENLAND SEA WATER

ELDEVIK ET AL.

PATHWAYS AND EXPORT OF GREENLAND SEA WATER

ELDEVIK ET AL.

PATHWAYS AND EXPORT OF GREENLAND SEA WATER

ELDEVIK ET AL.

PATHWAYS AND EXPORT OF GREENLAND SEA WATER

ELDEVIK ET AL.

PATHWAYS AND EXPORT OF GREENLAND SEA WATER

ELDEVIK ET AL.

PATHWAYS AND EXPORT OF GREENLAND SEA WATER

ELDEVIK ET AL.

PATHWAYS AND EXPORT OF GREENLAND SEA WATER

ELDEVIK ET AL.

PATHWAYS AND EXPORT OF GREENLAND SEA WATER

ELDEVIK ET AL.

PATHWAYS AND EXPORT OF GREENLAND SEA WATER

ELDEVIK ET AL.

PATHWAYS AND EXPORT OF GREENLAND SEA WATER

ELDEVIK ET AL.

PATHWAYS AND EXPORT OF GREENLAND SEA WATER

ELDEVIK ET AL.

PATHWAYS AND EXPORT OF GREENLAND SEA WATER

ELDEVIK ET AL.

PATHWAYS AND EXPORT OF GREENLAND SEA WATER

ELDEVIK ET AL.

PATHWAYS AND EXPORT OF GREENLAND SEA WATER

ELDEVIK ET AL.

PATHWAYS AND EXPORT OF GREENLAND SEA WATER

ELDEVIK ET AL.

PATHWAYS AND EXPORT OF GREENLAND SEA WATER

ELDEVIK ET AL.

PATHWAYS AND EXPORT OF GREENLAND SEA WATER

ELDEVIK ET AL.

PATHWAYS AND EXPORT OF GREENLAND SEA WATER

ELDEVIK ET AL.

PATHWAYS AND EXPORT OF GREENLAND SEA WATER

ELDEVIK ET AL.

PATHWAYS AND EXPORT OF GREENLAND SEA WATER

ELDEVIK ET AL.